JOURNAL OF MATERIALS SCIENCE 33 (1998) 4581–4588

Moisture-assisted crack growth at epoxy–glass interfaces

J. E. RITTER, J. R. FOX, D. I. HUTKO, T. J. LARDNER
Department of Mechanical and Industrial Engineering, University of Massachusetts, Amherst, MA 01003, USA

The double cleavage drilled compression (DCDC) test was used to measure the critical energy release rate, moisture-assisted crack growth, and fatigue threshold for epoxy–glass interfaces bonded with and without a silane coupling agent. The DCDC specimen consists of two glass beams (either soda-lime or fused silica) bonded together with an epoxy adhesive. A through-the-thickness hole is drilled in the centre of the specimen. In the DCDC test compressive loading causes tensile stresses to develop at the poles of the drilled hole. Cracks then nucleate in the epoxy–glass interface, extend from the poles, and propagate axially along the interface in primarily mode I loading. The resistance to moisture-assisted crack growth at untreated epoxy–glass interfaces is significantly less than that in monolithic glass specimens. However, the resistance to moisture-assisted crack growth at silane bonded epoxy–glass interfaces can be comparable with or greater than that in monolithic glass. Silane bonding of epoxy to glass is more effective with fused silica than soda-lime glass, with the fatigue limit of silane bonded epoxy–fused silica interfaces being about 2.5 times greater than that for silane bonded epoxy–soda-lime glass. These results are discussed in terms of possible interfacial crack growth mechanisms.

1. Introduction

Silane coupling agents are widely used to promote adhesion and moisture resistance of polymer adhesives bonded to glass [1–6]. These coupling agents have the general structure X_3–S_i–$(CH_2)_n$–Y, where $n = 0$–3, X is an hydrolysable group, e.g. $–OCH_3$, and Y is an organofunctional group, e.g. an amine group, that is selected for its reactivity with a given adhesive. It is generally believed that the X groups hydrolyse to silanol groups that then in turn react with the silanol groups on the glass surface to form primary Si–O–Si interfacial bonds. The Y groups can react with appropriate groups in the polymer adhesive to couple the adhesive to the glass. Silane coupling agents have been shown to enhance both the dry and wet adhesive strength of polymer adhesives to glass.

The purpose of this research is to study the effectiveness of silane coupling agents in improving the resistance of epoxy–glass interfaces to moisture-assisted crack growth. For this purpose the double cleavage drilled compression (DCDC) test was used to measure the fracture resistance of epoxy–glass (soda-lime and fused silica) interfaces with and without a silane coupling agent. The DCDC test was chosen because it has been shown that cracks tend to propagate in the interface even when the interfacial fracture toughness greatly exceeds the toughnesses of the adjoining materials [7] due to the stabilizing role of the compressive load.

2. Experimental procedure

The DCDC specimen geometry consists of a rectangular beam (about $6.0 \times 6.0 \times 60$ mm) with a hole (0.76 mm diameter) drilled into the centre (Fig. 1). Both monolithic soda-lime and fused silica glass specimens and epoxy–glass sandwich specimens were tested. For the monolithic glass specimens, the rectangular beams ($6.0 \times 6.0 \times 60$ mm) were cut from either a soda-lime or fused silica glass plate and the cut edges were polished with 240 grit silicon carbide paper. For the epoxy–glass sandwich specimens, two beams of glass ($3.0 \times 6.0 \times 60$ mm) were cut from the plates and then the beams were bonded together with an epoxy adhesive by pressing the bonded beam between stops that controlled the adhesive thickness to be 40 μm ($\pm$ 10 μm). To promote epoxy–glass adhesion, some of the sandwich specimens were treated with a silane coupling agent (3-aminopropyltriethoxysilane, 3-APES). For these specimens the glass was soaked for 3 h in the silane coupling agent prior to bonding with the epoxy. After curing the epoxy for 24 h in ambient air, the edges of the specimens were polished to eliminate any excessive adhesive that had squeezed out between the glass beams. A diamond core drill (radius 0.79 mm) was used to drill a hole through the centre of each specimen. All specimens were preconditioned in a high humidity environment (>95% relative humidity, r.h.) for 1 h prior to testing.

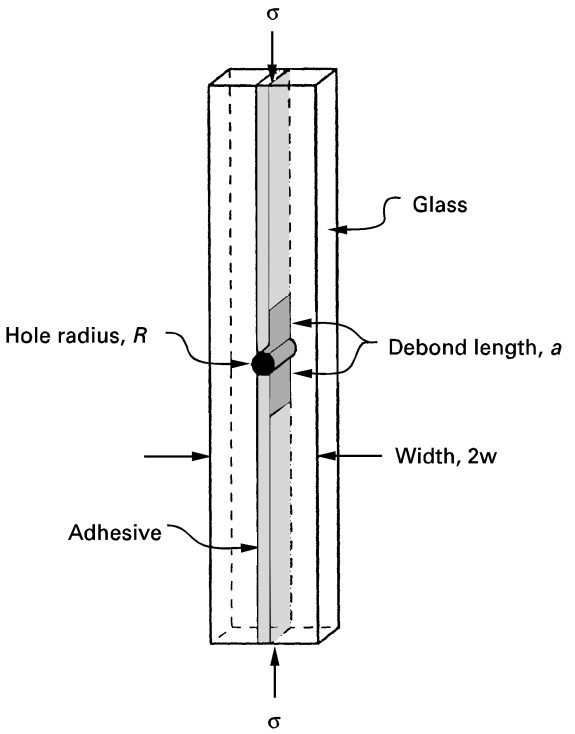

Figure 1 Schematic of the double cleavage drilled compression (DCDC) specimen.

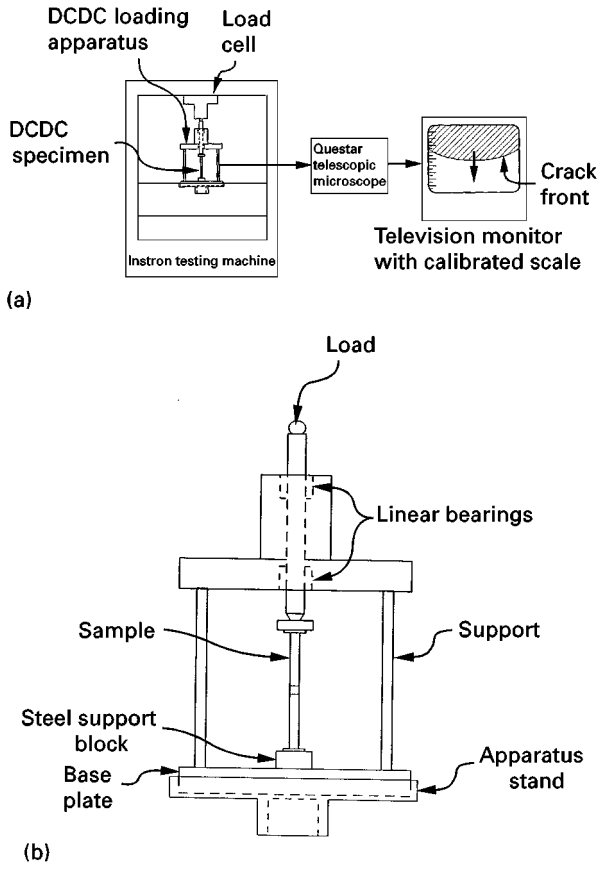

Figure 2 Schematic of (a) the DCDC test, and (b) the DCDC loading apparatus.

With the DCDC test, compressive loading causes tensile stresses to develop at the poles of the drilled hole. Cracks then nucleate, extend from the poles, and propagate axially along the interface in the sandwich specimens under primarily mode I loading. At a constant applied load, the energy release rate, G, diminishes upon crack extension, resulting in *stable crack growth*. The negative phase angle (a measure of the ratio of the shear stress to the normal stress at the crack tip) of a crack off the mid-plane causes the crack to propagate in the interface even when the interfacial fracture toughness greatly exceeds that of the adjoining glasses [7]. Finite element analysis [8] shows that the energy release rate, G, for a monolithic glass specimen is given by

$$\sigma\left(\frac{\pi R}{GE}\right)^{1/2} = \frac{w}{R} + \left(0.235\frac{w}{R} - 0.259\right)\frac{a}{R} \qquad (1)$$

where σ is the compressive stress, R is the hole radius, E is the elastic modulus, a is the crack length, and $2w$ is the specimen width. From Equation 1 it is seen that as a increases, G decreases. The phase angle ψ for the monolithic glass specimen is 0° [8], which corresponds to pure normal, i.e. mode I, loading at the crack tip. Because the adhesive layer is thin, G for the epoxy–glass sandwich is to a good approximation equal to that of the monolithic glass specimen [9, 10] and the phase angle, given by the asymptotic solution of Suo and Hutchinson [10], is -11°.

The compressive loading was applied in an Instron testing machine using graphite foil at the ends of the specimen to compensate for any surface roughness. All tests were carried out at high humidity (>95% r.h.) by enclosing the test fixture with a plastic envelope and then piping in moist air. After precracking to a crack length of about 3 mm, the load was slowly increased ($2\,\mathrm{kN\,min^{-1}}$) until the crack growth rate exceeded $10^{-5}\,\mathrm{m\,s^{-1}}$. The load was then held constant and crack growth was measured as a function of time using a Questar telescopic microscope, coupled with a television monitor (Fig. 2). An analysis of these data then gave the crack growth rate as a function of the applied G. The fracture toughness, G_c, of the glass and the epoxy–glass interfaces was measured by increasing the load until the precrack propagated catastrophically.

3. Results and discussion

Fig. 3a shows data for moisture-assisted crack growth for a soda-lime glass specimen where the crack grew continuously on the mid-plane of the specimen and was symmetric about the drilled hole. These data were typical for all the soda-lime and fused silica glass specimens tested. This continuous crack growth led to a steadily decreasing crack growth rate (velocity) as the crack grew into a decreasing G field with the velocity–G plot (Fig. 3b) showing very little scatter. In contrast, Fig. 4a shows moisture-assisted crack growth data for an untreated, i.e. no silane coupling agent, epoxy–soda-lime glass specimen. Although the crack grew on the interface and was symmetric about the drilled hole, the growth was irregular as the crack would intermittently arrest and then propagate ahead. This erratic stop–go crack growth leads to a relatively large scatter in the crack velocity data (Fig. 4b). This

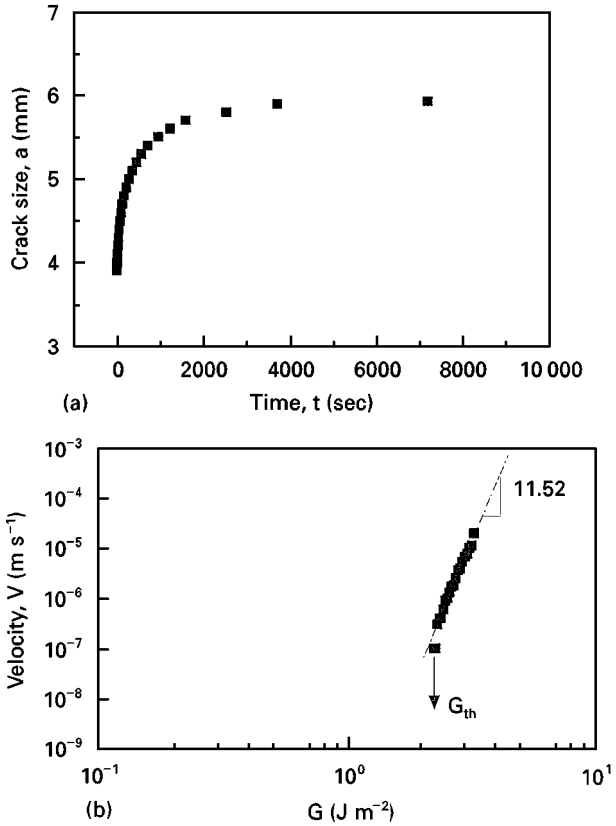

Figure 3 (a) Crack growth results for a soda-lime glass specimen, and (b) corresponding crack growth rates as a function of the energy release rate.

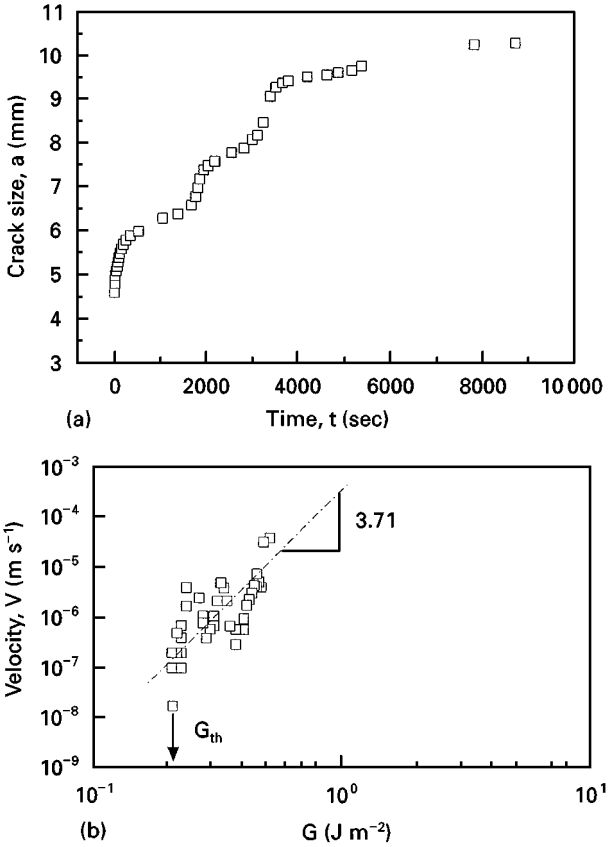

Figure 4 (a) Crack growth results for an untreated epoxy–soda-lime glass specimen, and (b) corresponding crack growth rates as a function of the energy release rate.

crack growth behaviour was typical for all the epoxy–glass specimens. Finally, it should be noted that the arrows in Figs 3b and 4b indicate the threshold energy release rate, G_{th}. At G_{th} no measurable crack growth occurred within 2–3 h for the glass specimens, but with the epoxy–glass specimens, crack healing occurred, i.e. the crack front began to retract.

Fig. 5 compares the crack growth rate (velocity data measured for monolithic soda-lime glass with that for the untreated epoxy and soda-lime glass interface and Fig. 6 compares the crack velocity data for fused silica glass with that for the untreated epoxy–fused silica glass interface. The monolithic glass data in Figs 5 and 6 agree well with previous DCDC data [11–13] and double cantilever beam (DCB) data [14, 15]. All sets of data in Figs 5 and 6 were fitted to a power law relationship given by

$$V = AG^{n} \tag{2}$$

where V is crack velocity, and A and n are constants. The exponent n is most significant because it is a measure of the sensitivity of crack growth to the applied G; a higher n signifies a greater resistance to "stress-corrosion" crack growth. It is evident that the untreated epoxy–glass interface is much less resistant to moisture-assisted crack growth than the corresponding monolithic glass. Both the G necessary for crack growth and the power law exponent n are considerably greater for monolithic glass. It can also be seen in Figs 5 and 6 that the experimental scatter in the crack velocity data for the untreated epoxy–glass

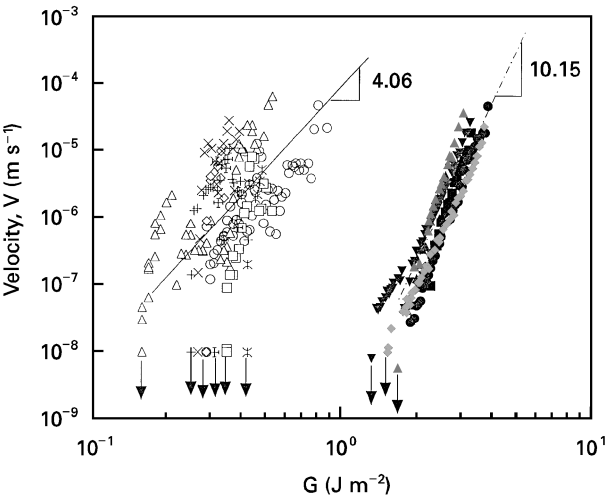

Figure 5 Comparison of moisture-assisted crack growth rates in soda-lime glass (closed symbols) to that at untreated epoxy–soad-lime glass interfaces (open and "cross-hatched" symbols) where the different symbols indicate individual samples.

interface is considerably greater than for monolithic glass. This scatter is due to both that observed on a single specimen and that observed between multiple samples. The crack velocity scatter observed in a single untreated epoxy–glass specimen is simply a consequence of the "stop–go" crack growth, see Fig. 4b. The "between-specimen" scatter in the untreated epoxy–glass samples is undoubtedly due to microstructural variability in the epoxy that leads to

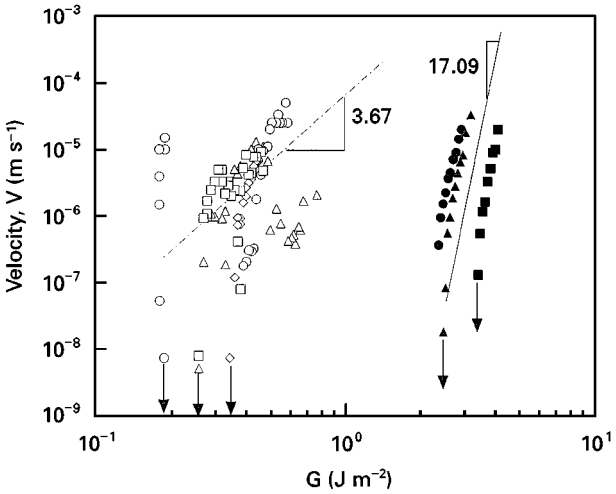

Figure 6 Comparison of moisture-assisted crack growth rates in fused silica glass (closed symbols) to that at untreated epoxy–fused silica glass interfaces (open symbols) where the different symbols indicate individual samples.

variability in the interfacial bonding. Finally, by comparing Figs 5 and 6 it can be seen that the crack velocity data for the untreated epoxy–soda-lime glass interface is essentially the same as for the untreated epoxy–fused silica interface.

It is believed that for the untreated epoxy–glass interface, the high surface energy of the glass attracts water molecules to the crack tip where they then displace the epoxy molecules that are physically adhered through secondary bonding to the glass surface [2, 16, 17]. This displacement occurs even in the absence of an applied stress [2]; however, a stress at the crack tip strains these interfacial secondary bonds and makes them more susceptible to water, hence, the dependency of crack velocity on G. Based on the results in Figs 5 and 6, the composition of the glass has an insignificant effect on the secondary bonding between the epoxy and glass. In contrast, for monolithic glass the water molecules have to break the strained primary Si–O–Si bonds at the crack tip [18]. The fact that soda-lime glass is less resistant (lower n) to "stress-corrosion" crack growth than fused silica is thought to be related to the cations that disrupt the Si–O bonds in the glass network, making soda-lime glass less viscous and more soluble in water. Fig. 7 illustrates these "stress-corrosion" mechanisms for an untreated epoxy–glass interface and for a silicate glass. The considerably lower G and n values (about 4) for crack growth along the untreated epoxy–glass interface are undoubtedly related to the ease by which secondary bonds between the epoxy and glass can be broken.

Fig. 8 compares the crack growth rate data for silane bonded epoxy–soda-lime glass interfaces with that for monolithic soda-lime glass and Fig. 9 makes a similar comparison but with silane bonded epoxy–fused silica glass and monolithic fused silica glass. By comparing these results to those in Figs 5 and 6, it is evident that the silane coupling agent significantly increases the resistance of the epoxy–glass interface to moisture-assisted crack growth. For the

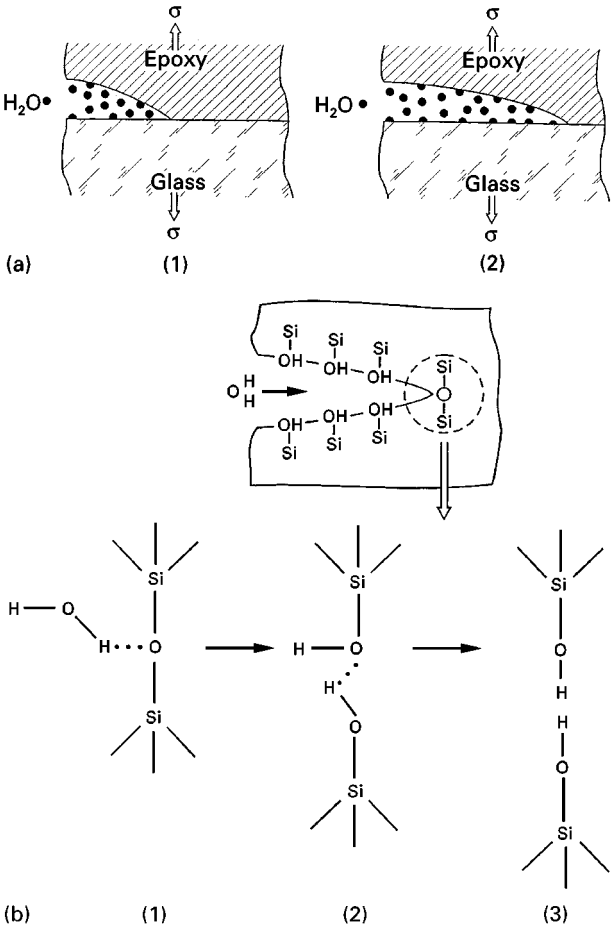

Figure 7 Schematic of the moisture-assisted crack growth (a) untreated epoxy–glass interface where the water molecule is preferentially absorbed on the glass surface in place of the epoxy molecule (after [16]); and (b) silicate glass where the water molecule breaks the strained Si–O bond at the crack tip (after [18]).

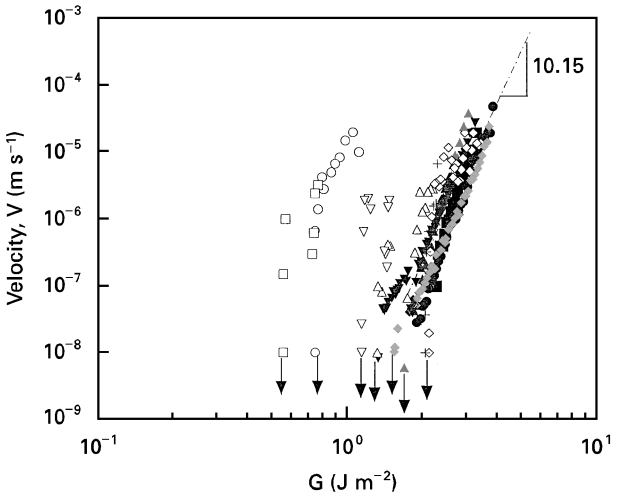

Figure 8 Comparison of moisture-assisted crack growth rates in soda-lime glass (closed symbols) to that at silane bonded epoxy–soda–lime interfaces (open symbols) where the different symbols indicate individual samples.

silane bonded epoxy–soda-lime glass interface, both n and the G necessary for crack growth can become comparable with that required for the monolithic soda-lime glass; whereas, for the silane bonded epoxy–fused silica interface, the G for crack growth

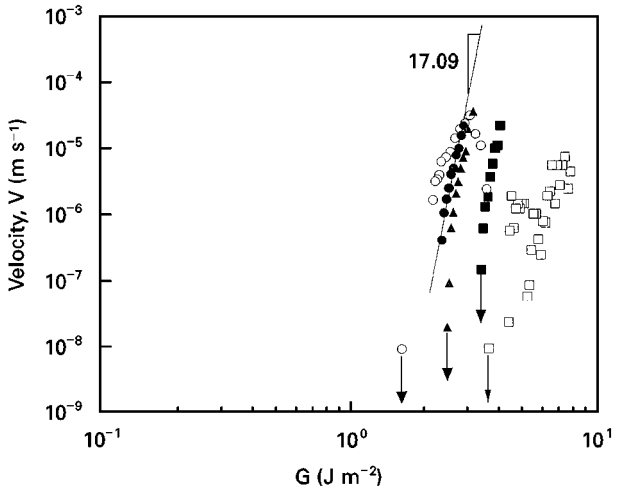

Figure 9 Comparison of moisture-assisted crack growth rates in fused silica glass (closed symbols) to that at silane bonded epoxy–fused silica interfaces (open symbols) where the different symbols indicate individual samples.

can become greater than that required for crack growth in the monolithic fused silica glass. In fact, in three of the five silane bonded epoxy–fused silica specimens tested, cracks initiated off centre from the drilled hole and propagated parallel to the interface but entirely in the fused silica, indicating that the fracture toughness of the interface was greater than that of monolithic fused silica. This will be discussed further below. The increase in the resistance of the silane bonded epoxy–glass interface is undoubtedly due to the epoxy being chemically bonded to the glass via the silane coupling agent. Because crack growth in these samples was truly interfacial (neither scanning electron microscopy or X-ray photoelectron spectroscopy revealed any epoxy adhered to the glass surface after crack growth), we believe that this moisture-assisted crack growth occurred by rupturing the Si–O bonds formed by the silane coupling agent, similar to the mechanism illustrated in Fig. 7b for monolithic silicate glass.

Fig. 10 illustrates in a rather simplified manner how silane molecules are thought to bond themselves to the glass surface and the epoxy adhesive [1–5]. First, the silane coupling agent, in this case 3-APES, is hydrolysed and the hydroxyl groups then react with the hydroxyl groups on the glass surface to form primary Si–O bonds across the interface. Once the silane molecule is attached to the glass surface via Si–O–Si primary bonds, the NH_2 end groups of the attached silane molecules react with the epoxy resin to adhere the epoxy via primary bonds to the glass surface. Note that the remaining epoxide groups will react with the diamine hardener (not shown in Fig. 10) to form the epoxy network. It is the flexibility of the silane molecule that we believe helps relieve the strained Si–O–Si bonds at the interface and, thereby, decrease the susceptibility of the interfacial Si–O–Si bonds to moisture attack. Although the silane coupling agent could ideally react with every hydroxyl group present on the glass surface, steric hinderance will prevent this [17]. Also, it is quite likely that the silane molecules will cross-link between themselves [13]. These latter two effects will lead to a variability in the density of the interfacial Si–O–Si bonds across the interface, as well as, in the flexibility of the silane molecule itself. It is these effects that we believe lead to the "between-sample" scatter in the silane bonded epoxy–glass specimens being considerably greater than that observed with the untreated epoxy–glass specimens. Finally, this simple model for silane bonding also explains why the silane bonding to soda-lime glass is less effective than to fused silica. Previous research [17, 19, 20] has shown that there is an enrichment of sodium ions in the glass surface when soda-lime glass is exposed to water. These sodium ions form cationic bonds with the surrounding water molecules, see Fig. 11, which can then block the silane molecule from attaching to the glass surface [17]. Admittedly, further research is needed to prove these hypotheses conclusively and to determine the optimum conditions for bonding epoxy to glass via a silane coupling agent.

Table I summarizes the average threshold, G_{th}, and critical, G_c, energy release rates for the various monolithic glass and epoxy–glass specimens. Consistent with the moisture-assisted crack growth data in Figs 5 and 6, G_{th} and G_c for the untreated epoxy–glass interface are considerably less than those for the monolithic glasses. On the other hand, G_{th} and G_c for the silane bonded epoxy–soda lime glass interface are comparable with monolithic soda-lime glass and for the silane bonded epoxy–fused silica glass interface are somewhat greater than monolithic fused silica. This is consistent with the respective crack growth rate data in Figs 8 and 9. Finally, it should be recognized that although moisture-assisted crack growth rates at epoxy–glass interfaces can be characterized in terms of the energy release rate, the large variability observed in the crack velocities makes finite life prediction too uncertain. Instead, we believe that epoxy–glass interfaces should be designed based on the energy release rate necessary to initiate moisture-assisted crack growth, i.e. G_{th}.

As mentioned above, cracks in the silane bonded epoxy–fused silica specimens had a tendency to initiate and propagate parallel to the interface but entirely in the fused silica glass. For the crack to propagate in the glass and off-centre of the axis of the specimen, the energy release rate for the substrate crack, G, must be greater than the fracture toughness of the fused silica, G_c, i.e. $G > G_c$, and the energy release rate for the interface crack, G_i, must be less than the fracture toughness of the interface, G_{ci}, i.e. $G_i < G_{ci}$. It follows then that [21]

$$G_{ci} > G_c\left(\frac{G_i}{G}\right) \tag{3}$$

From Fig. 12 it can be seen that the crack in the glass is off-set by an amount b equal to b/R of about 0.2, where R is the hole radius. From the analysis of He *et al.* [8] we estimated that the ratio of G_i/G to be about 1.8 for an off-set of 0.2. Based on Equation 3 this

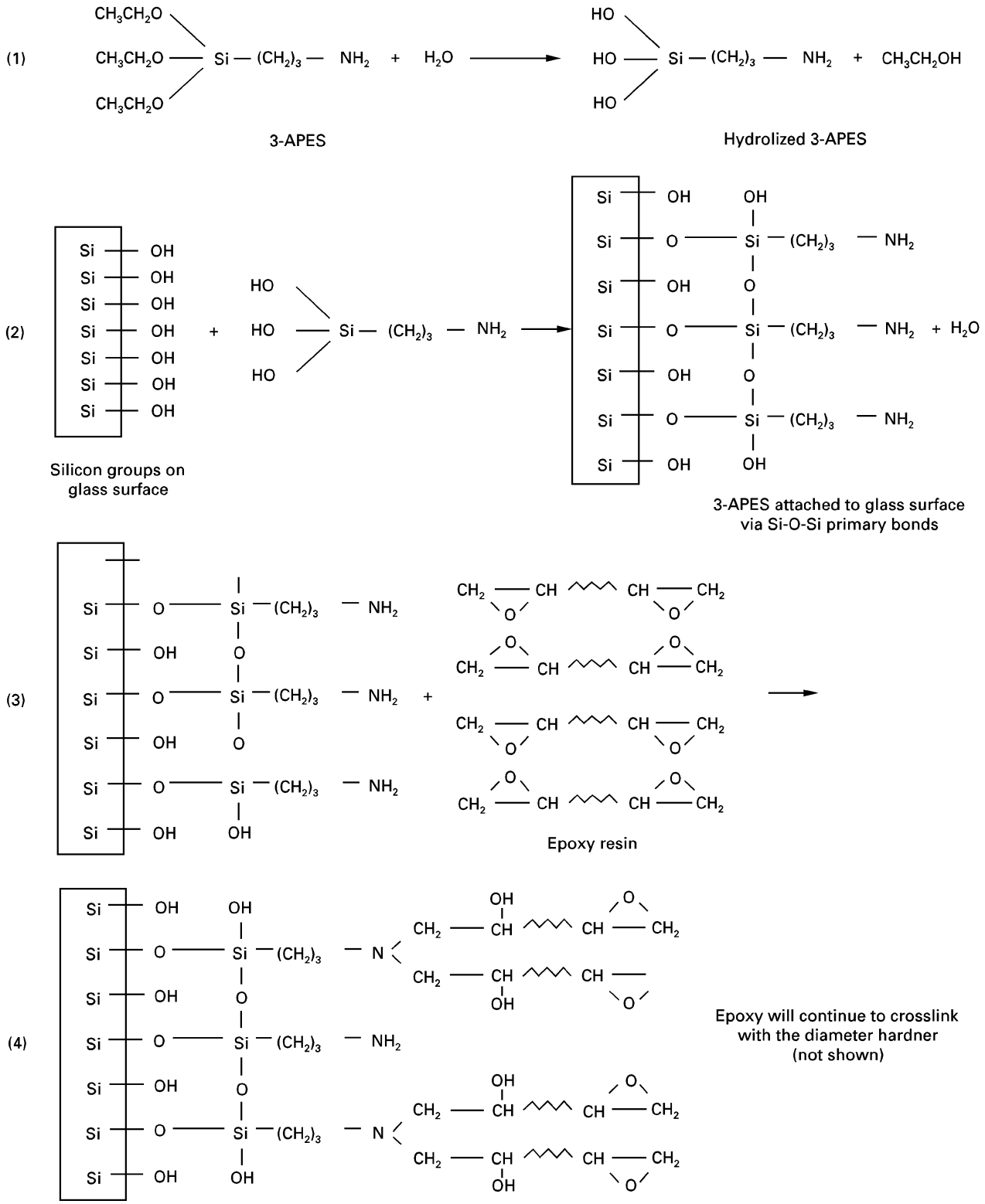

Figure 10 Schematic of the chemical reaction steps used to bond 3-aminopropyltriethoxysilane (3-APES) molecules to the glass surface and epoxy.

would give for these silane coupled epoxy–fused silica glass interfaces a $G_{ci} > 14.2\,J\,m^{-2}$. This interfacial fracture energy can be compared with that calculated by multiplying the number of possible interfacial Si–O bonds per unit area by the Si–O bond energy [20]. The maximum density of the interfacial Si–O bonds per square metre can be estimated from the density of OH groups on a hydrated silica surface, which has been given as 5×10^{18} [17]. Taking the Si–O bond energy to be $890\,kJ\,mol^{-1}$ [22], a fracture energy of $7.4\,J\,m^{-2}$ is calculated. This value is in good agreement with that measured for monolithic glass and the silane bonded epoxy–glass interfaces, see Table I. What makes it possible for silane bonded epoxy–glass interfaces to have fracture energies greater than that estimated from breaking primary Si–O bonds is that the silane molecule can deform and absorb additional energy.

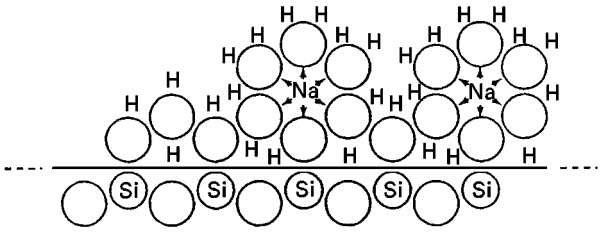

Figure 11 Schematic of sodium ions on the soda-lime glass surface that form cationic bonds with H_2O molecules (after [17, 18]).

TABLE I Summary of the threshold, G_{th}, and critical G_c, energy release rates

Specimen	G_{th}(J m^{-2})	G_c(J m^{-2})
Soda-lime glass (SLG)	1.69($\pm$0.38)	8.17($\pm$0.78)
Fused silica (FS)	2.76($\pm$0.57)	7.89($\pm$1.69)
Untreated epoxy–SLG interface	0.25($\pm$0.07)	2.01($\pm$0.56)
Untreated epoxy–FS interface	0.26($\pm$0.10)	2.37($\pm$0.30)
Silane coupled epoxy–SLG interface	1.32($\pm$0.65)	8.79($\pm$0.76)
Silane coupled epoxy–FS interface	3.31($\pm$1.56)	8.89($\pm$0.71)

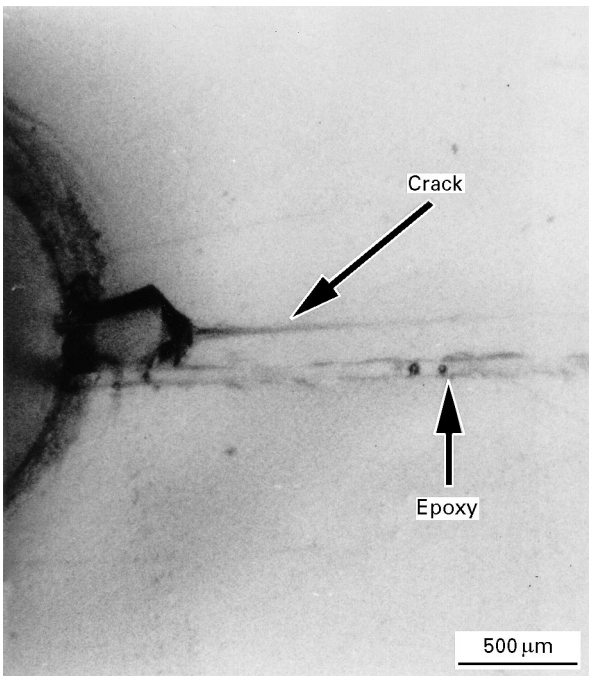

Figure 12 Crack initiated and propagated in the fused silica glass substrate rather than the silane bonded epoxy–fused silica glass interface.

Previously we have measured moisture-assisted crack growth for untreated epoxy–soda-lime glass interfaces [9, 16] using the interfacial four-point flexure experiment where the phase angle $\psi = 30^\circ$. To see if there is an influence of phase angle on moisture-assisted crack growth, Fig. 13 compares the crack growth rates as measured by the DCDC test (Fig. 5) to that determined previously [9, 16] by the interfacial four-point flexure test. Note that G is normalized by

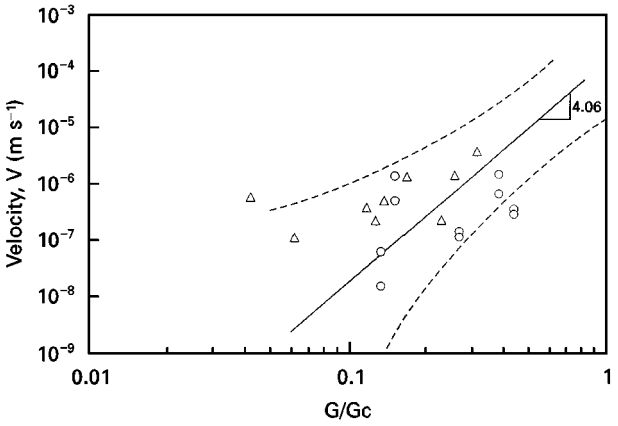

Figure 13 Comparison of moisture-assisted crack growth rates in untreated epoxy–soda-lime glass interfaces as measured by the DCDC test ($\psi = -11^\circ$) to that measured by the interfacial four-point flexure test ($\psi = 30^\circ$) [19, 16]. (——) DCDC best-fit line through the epoxy–glass data in Fig. 5, (– – –) $\pm$ one standard deviation of this fit. Four-point flexure from (○) [16], (△) [9].

the critical energy release rate, G_e, of the interface because we find that over time, different batches of epoxy from the same supplier can exhibit different G_c's. From [9], G_c was 3.36 ($\pm$1.59) J m^{-2} compared with a G_c of 8.5 ($\pm$3.5) J m^{-2} from [16] and with a G_c of 2.01 ($\pm$0.56) J m^{-2} as determined by this research using the DCDC test. It is evident from Fig. 13 that the phase angle (-11 versus 30°) has a negligible influence on the crack growth rates within experimental scatter. This agrees with our previous research where we saw no influence of phase angle from 13 to 54° on moisture-assisted crack growth [9].

4. Conclusions

The DCDC test offers several distinct advantages for measuring crack growth at polymer–glass interfaces, including experimental simplicity of compressive loading, ease of precracking, mid-plane crack stability, and stable crack growth. This gives the test the unique advantage of being able to measure the critical energy release rate, subcritical crack growth, and the fatigue threshold in the same specimen. Especially important is being able to determine the fatigue threshold because this is the parameter that should be used in engineering design of adhesive joints subject to subcritical crack growth. Based on the results from the DCDC tests of epoxy–glass interfaces, we believe that the mechanism of moisture-assisted crack growth at an untreated epoxy–glass interface differs significantly from either a silane bonded epoxy–glass interface or monolithic glass, both of which are considerably more resistant to crack growth than the untreated epoxy–glass interface. For a silane bonded epoxy–glass interface or monolithic glass, water at the crack tip must break primary Si–O–Si bonds rather than the secondary bonds that exist at an untreated epoxy–glass interface. Silane bonding of epoxy to fused silica glass is more effective than to soda-lime glass because the cations at the surface of the soda-lime glass can bond with surrounding water molecules

that prevent the bonding of the silane molecule to the glass surface.

Acknowledgements

This research was supported by NSF Grants DMR-9301761 and DMR-9703667.

References

1. S. WU, "Polymer interface and adhesion" (Marcel Dekker, New York, 1982).
2. A.J. KINLOCH, "Adhesion and adhesives: science and technology" (Chapman and Hall, London, 1987).
3. E. P. PLUEDDEMANN, "Silane coupling agents", 2nd Edn (Plenum Press, New York, 1991).
4. A. J. KINLOCH, Preprint No. 08, Proceedings of the Institution of Mechanical Engineers, London, 1996.
5. R. LIN, H. WANG, D. S. KALEKA and L. S. PENN, *J. Adhesion Sci. Technol.* **10**(4) (1996) 327.
6. R. LIN, R. P. QUICK, J. KUANG and L. S. PENN, *ibid.* **10**(4) (1996) 341.
7. M. R. TURNER, B. J. DALGLEISH, M. YITTE and A. G. EVANS, *Acta Metall. Mater.* **43** (1995) 3459.
8. M.Y. HE, M. R. TURNER and A. G. EVANS, *ibid.* **43** (1995) 3453.
9. J. E. RITTER, T. J. LARDNER, A. J. STEWART and G. C. PRAKASH, *J. Adhesion* **49** (1995) 97.
10. Z. SUO and J. W. HUTCHINSON, *Mater. Sci. Enging* **A107** (1989) 135.
11. C. JANSSEN, in Proceedings of the Tenth International Congress on Glass, Kyoto, Japan, July, 1974 (The Ceramic Society of Japan, Kyoto, Japan, 1974) pp. 23–30.
12. W. H. SMITH, *Closed Loop Magazine* **Spring** (1987) 18.
13. J. D. HELFINSTINE, S. T. GULATI and D. G. PIKLES, in "The Physics of Non-Crystaline Solids", edited by L. D. Pye, W. C. LaCourse and H. J. Stevens (Taylor and Francis, Bristol, PA, 1992) pp. 654–8.
14. S. W. WIEDERHORN, *J. Amer. Ceram. Soc.* **50** (8) (1969) 407.
15. S. M. WIEDERHORN and L. H. BOLZ, *ibid.* **53** (10) (1970) 543.
16. J. E. RITTER, T. J. LARDNER, W. GRAYESKI, G. C. PRAKASH and J. LAWRENCE, *J. Adhesion* **63** (1997) 265.
17. R. K. ILER, "The chemistry of silica" (Wiley, New York, 1975).
18. T. A. MICHALSKE and S. W. FREIMAN, *J. Amer. Ceram. Soc.* **66** (1953) 284.
19. C. G. PATANO, D. B. DOVE and G. Y. ONODA, *J. Vac. Sci. Technol.* **13** (1) (1976) 414.
20. T. A. MICHALSKE and E. R. FULLER JR, *J. Amer. Ceram. Soc.* **68** (11) (1985) 586.
21. M.-Y. HE and J. W. HUTCHINSON, *Int. J. Solids Structures* **25** (9) (1989) 1053.
22. R. H. DOREMUS, "Glass science" (Wiley, New York, 1973).

Received 23 September 1997
and accepted 11 May 1998